Journal of Metals, Materials and Minerals, Vol.22 No.1 pp. 87-97 ,2012

A Micromechanical Flow Curve Model for Dual Phase Steels

Sawitree SODJIT and Vitoon UTHAISANGSUK*

Department of Mechanical Engineering, Faculty of Engineering,
King Mongkut's University Technology Thonburi, Bangkok, Thailand

Abstract

In the automotive industries, Dual Phase (DP) steels have become a favoured material for the car body parts due to their excellent combination of high strength and good formability. A microstructure of DP steel generally consists of a matrix of ferrite reinforced by small islands of martensite. Experimental investigations showed that effects of martensite phase fraction, morphology, and phase distribution play an important role for the mechanical and fracture behaviours of the dual phase steel. In the present work, an approach concerning FE based modelling for predicting flow curve of DP steels has been introduced using a Representative Volume Element (RVE). Two dimensional RVE models were prepared on microstructural level using micrographs of the investigated DP steels having different martensite phase fractions. The applied physical flow curve models of the individual single phases are based on dislocation theory and take into account the local chemical compositions. The models also include phase boundary dislocation (PBD) density, which accumulates at the phase boundaries due to the austenite-martensite transformation during quenching process. These dislocations contribute to both an increase in forest dislocations and a building up of back stresses. The calculated stress-strain curves for the DP steels were verified with experimental results determined from tensile tests. Furthermore, the micromechanics based model was used to describe the local stress and strain development of the individual phases in the DP microstructures. By this manner, an optimization of the dual phase high strength steel with respect to its microstructural constituents is possible.

Keywords: Dual phase steel, Flow curve, Microstructure, Representative volume element, Phase boundary dislocation.

Introduction

In recent years, there has been growth in the search and use of new advanced materials in the automotive industry. The concept development in the automobile industry is generally concerned with such important factors, for example, the customer expectations like fuel consumption, design, performance, low cost usage, and legal requirements as well as standards for crash, passive safety features, and low greenhouse gas emission. To ensure the position of steel, the world leaders in steel production started a research program to achieve the ULSAB (Ultra-Light Steel Auto Body).(1) It means that different parts in a vehicle need to be as light as possible, but still exhibit a sufficient strength. Thus, the advanced high strength Dual Phase (DP) steel has attracted more interest because of its excellent combination of high strength property and good formability. (2)

Dual phase steels are low carbon micro-alloyed steels. The microstructures of DP steels consist of hard martensite islands distributed in soft ferritic matrix. In general, they have a purely ferrite matrix and about 5 - 30 percent volume fraction of martensite dispersed in patches as a second phase. Hereby, DP steels have characteristic mechanical properties which include low yield strength and high ultimate tensile strength when comparing with other conventional low-carbon steels. The overall mechanical properties of DP steels depend not only on the intrinsic properties of ferrite and martensite themselves, but also on the

E-mail: Hvitoon.uth@kmutt.ac.thH Tel: +66 2470 9274; Fax: +66 2470 9111

microstructural features such as volume fraction and morphology of martensite. The finer the grain size, the higher are the strength and the volume fraction of the martensitic phase principally increases the tensile strength of the DP steels. However, higher volume fraction of the martensitic phase reduces the ductility of the DP steels.(3) To design an optimal combination of strength and deformation, a right description of the material behaviour is necessary. At present, in most FE based simulations of industrial forming operations, the microstructure of multiphase steels is not considered, which actually is the most important parameter controlling their overall mechanical properties.(4)

In this work, DP steels with different martensite contents and morphologies were produced by means of the intercritical annealing at different temperatures. Afterwards, the metallographic investigations and tensile tests were carried out for characterizing the produced DP steels. In order to investigate the influence of the multiphase microstructure on the deformation behaviour, micrographs of these steels taken from the Light Optical Microscopy (LOM) were applied for generating 2D Representative Volume Elements (RVEs). The individual phases in the RVE were considered separately, in which different flow curves based on dislocation theory and chemical compositions were given. The dislocations accumulating at the phase boundaries between transformed martensite and ferrite were taken into account as an additional term in the flow curve model of ferrite. The RVE simulations were used to calculate the macroscopic flow curves of the DP steels and then to study effect of microstructure morphologies on the predicted curve.(5) To verify the introduced flow curve models experimental determined and FE numerical predicted stress-strain responses were compared.

Materials and Experimental Procedures

Materials

The steel sheet samples with DP microstructures were obtained through laboratory heat treatment. The as-received material was a hot-rolled strip with a thickness of 3.6 mm that was cut to a rectangular sheet with the dimension of 50x100 mm^2. The chemical composition of the investigated steel was firstly determined using vacuum emission spectroscopy and the result is shown in Table 1. Then, the steel sheets were pickled by a solution of 20% HCl in water at the temperature of 80°C. The steel sheets were rolled at room temperature using a twin rolling mill in order to obtain a final thickness of 1.2 mm. This thickness reduction is approximated according to a cold-rolling degree of 65%. Subsequently, specimens for the tensile test were prepared parallel to the rolling direction. The metallographic examination of the as-received steel showed a ferrite-pearlite microstructure, as illustrated in Figure 1.

Table 1 : Chemical composition of the investigated steels,mass contents %.

Material	C	Si	Mn	P	S	Cr	Nb	Cu
annealed DP	0.090	0.012	1.340	0.013	0.003	0.020	0.002	0.010
DP600	0.172	0.252	1.387	0.019	0.010	0.553	0.019	0.010
DP800	0.110	0.639	2.132	0.015	0.004	0.000	0.020	0.00

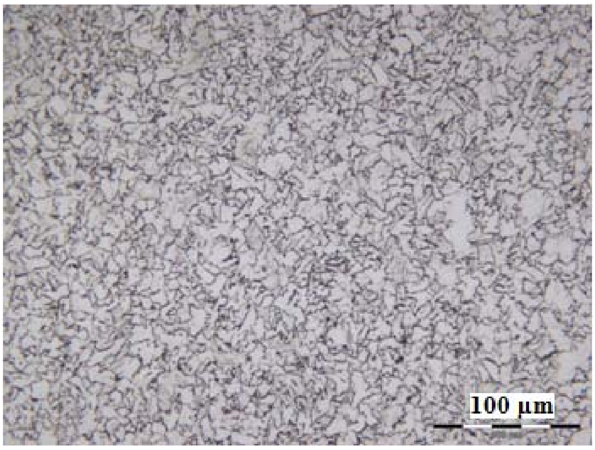

Figure 1 : Microstructure of the as-received steel sheet.

Heat Treatment

A laboratory heat treatment was performed for the prepared specimens in order to produce DP microstructure. The intercritical annealing at different temperatures was carried out for obtaining steel samples with DP microstructures containing different martensite phase fraction and corresponding ferrite grain sizes. The heat treatment experiments were conducted in salt bath, for which a salt composition of 78% $BaCl_2$ and 22% NaCl was used. The two-phase temperature regions for the experiment were previously calculated using ThermoCalc according to the equilibrium condition. The sheets samples were immersed in the salt bath at five different temperatures of 750, 770, 790, 810, and 830°C. These temperatures lie between the A_{c1} and A_{c3} temperature of the investigated steel so that it just had an austenitic-ferritic structure. The holding time after reaching each intercritical temperature was 5 min. Finally, the samples were directly quenched in water to room temperature, by which the phase transformation of austenite to martensite occurred. The produced DP microstructures exhibited the Martensite Phase Fraction (MPF) of 25, 35, 45, 60, and 90% with regard to the intercritical annealing temperatures of 750, 770, 790, 810, and 830°C, respectively.

Mechanical Testing

After annealing in salt bath, tensile specimens according to DIN EN 50114 were cut from the heat-treated steel sheets. Here, the sub-size tensile sample with a nominal gauge length of 25 mm and nominal width of 5 mm was used. These specimens were elongated under uniaxial condition on a universal testing machine, which was equipped with an automatic controller using displacement control mode. A cross-head speed of 0.04 mm/s that is corresponded to a quasi-static strain rate of 0.002 s^{-1} was applied. Three replicated specimens for each DP microstructure with different MPFs were tested. During the tensile experiments, force and displacement were recorded using an extensometer. From these data, conventional stress and strain values could be calculated. The reproducibility of the determined stress-strain curves was acceptable and necking was mostly observed inside the gauge length of all tested samples. The resulted true stress-true strain curves from the tensile tests are presented in Figure 2 for different annealed DP steels. The stress-strain curves of a commercial DP600 and DP800 steel were also compared in the same graph. The ultimate tensile strength, yield strength and uniform elongation averaged from three replicated tensile tests are given together with the respective martensitic phase fractions and intercritical temperatures in Table 2.

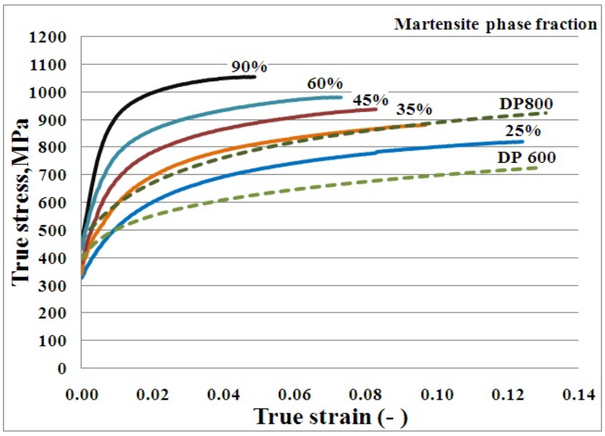

Figure 2. Results of tensile tests for different annealed DP steels in comparison with commercial DP600 and DP800 steel.

Material	IAT (°C)	Phase fraction (%)	YS (MPa)	UTS (MPa)	Uniform elongation (%)
	750	25	337	814	12.0
	770	35	345	888	9.2
annealed DP	790	45	363	933	7.6
	810	60	432	957	7.1
	830	95	456	1048	5.2
DP 600	-	35	393	720	13.2
DP 800	-	40	457	923	13.5

Table 2 : Mechanical properties of the investigated DP steels.

Microstructure Analysis

Samples for the metallographic analysis were prepared from the specimens after tensile test from the region undergoing minimum deformation. In this case, it was the area of the sample shoulder. The sample were grounded using silicon carbide paper with a grit size of 240, 400, 600, 1000 and 1200 in sequence, and were then polished with 1 µm and 0.03 µm alumina, respectively. After polishing, the specimens were pre-etched with a 2% Nital solution (2 ml HNO_3 in 98 ml ethanol) for 3-5 seconds and followed by a 5% $Na_2S_2O_5$ (5 g $Na_2S_2O_5$ in 95 ml distilled water) about 10-15 seconds for tint-etching. The phase fraction and grain size of each specimen were characterized according to ASTM E562 and E112-46, respectively. The measurement of the phase fraction was based on percent of area fraction. Figure 3 shows all investigated DP microstructures with different martensite phase fractions. In the micrographs the bright gray zones are ferritic phase and the dark gray regions are martensitic phase.

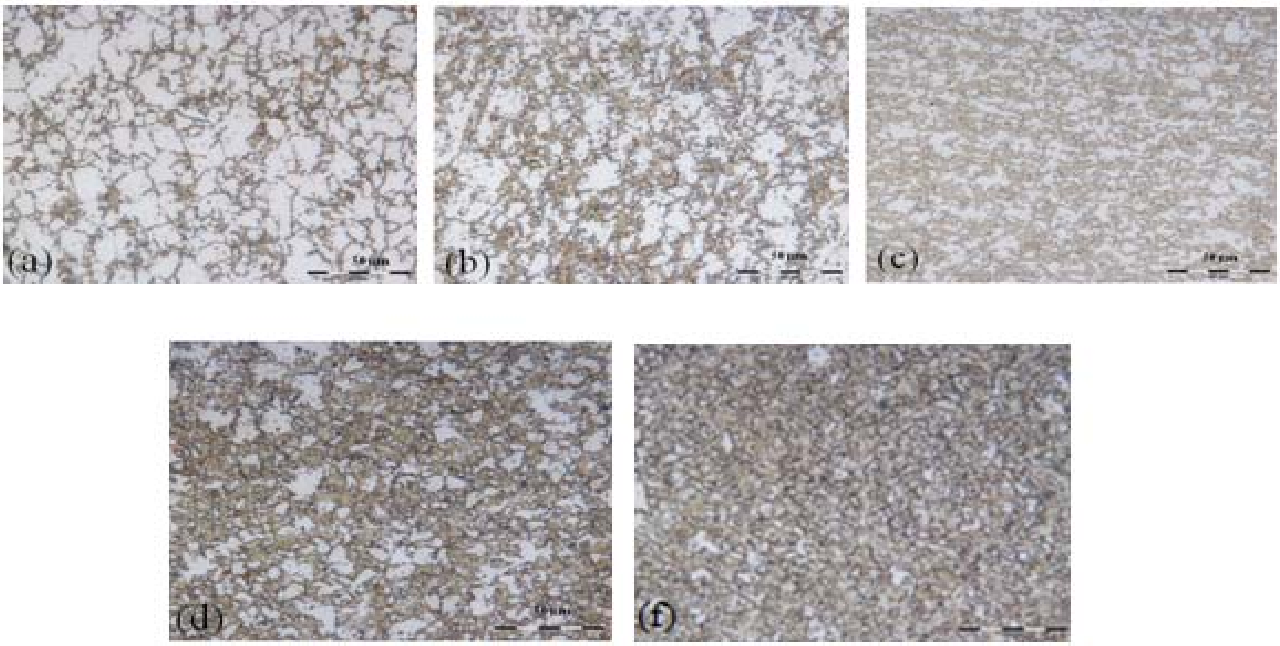

Figure 3 : Optical micrographs of the investigated DP steels with the MPF of (a) 25%, (b) 35%, (c) 45%, (d) 60%, and (f) 90%.

Micromechanical FE Modeling

Representative Volume Element

Generally, description of the mechanical behavior of steel was done using continuum mechanics on the so-called macro-scale. On this scale the entire material is treated as a continuum, whereas on the microstructure level, or the so-called meso-scale, the high strength steel is clearly discontinuous because of its multiphase character. Thus, the assumption of homogeneity and continuity is only valid on the macro-scale. The determination of macroscopic mechanical properties can be interpreted as an averaging over the microstructure volume elements. Such an element is called a Representative Volume Element (RVE). A RVE exhibits both phase composition and microstructural configuration. The RVE can be simply identified as a cut-out of the macroscopic material. It needs to be large enough for representing most important microstructure features of the investigated material. Besides, it should be small enough to provide homogeneous overall stress and strain value. By applying the RVE method, stress and strain distribution of each constituent phases and their contribution to the overall macroscopic strength of material can be obtained. For defining a RVE model, assumptions for the complexity in form and distribution of the containing phases are necessary. For example, in case of a two phase microstructure with spherical second phase inclusions in surrounding matrix, a simplest assumption is that the second phase distribution is homogenous, periodic and globular. Note that three steps have to be considered for the calculation of the overall strain hardening behavior of dual phase microstructures by means of the RVE method:

(a) Geometric definition of the RVE, which embodies the essential features of the microstructure.

(b) Constitutive description of the mechanical behavior of each phase.

(c) Homogenization strategy for obtaining macroscopic mechanical behavior.

To what extent the RVE can describe the behavior of material depends in such a way on how accurately the RVE captures the morphological features of the actual microstructure. However, the calculation accuracy and model simplification show oppositional requirements in this context.[6]

In this work, a 2D RVE model has been applied. For the RVE simulation an appropriate model and material properties data must be prepared firstly. Micrographs of the investigated dual phase microstructures were converted to a 2D FE model. By this manner, microstructure morphologies and amount of martensite and ferrite could be taken into account. An example of the 2D RVE model generated from real DP microstructure is shown in Figure 4, which was used for further FE calculations. The FE simulations were performed using ABAQUS and the flow behaviors of DP steels were afterwards determined.

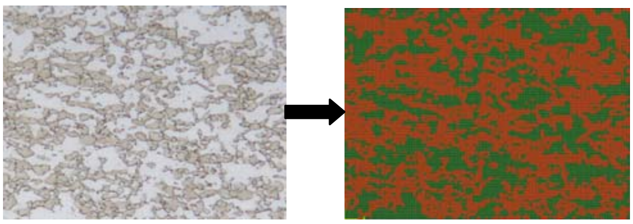

(a) (b)

Figure 4: (a) Micrograph of the investigated DP microstructure with MPF of 45% and (b) corresponding generated 2D RVE model with 130x170 elements.

Microstructure Based Flow Curve Model

A dislocation based strain hardening approach was used to describe the flow curve of the containing individual phases.[7] According to this approach the effective stress-strain can be described as

$$\sigma = \sigma_0 + \Delta\sigma + \alpha \cdot M \cdot \mu \cdot \sqrt{b} \cdot \sqrt{\frac{1-\exp(-M k_r \varepsilon)}{k_r \cdot L}} \qquad (1)$$

where σ is the flow stress at a true strain of ε. The descriptions of each term are given in detail below and the values for each parameter were taken from earlier works [8]. The first term σ_0 represents the Peierls stress and effects of alloying elements in solid solution on Peierls stress is shown as following:

$$\sigma_0 \text{ (in MPa)} = 77 + 750\,(\%P) + 60\,(\%Si) + 80(\%Cu) + 45\,(\%Ni) + 60\,(\%Cr) + 80\,(\%Mn) + 11\,(\%Mo) + 5000\,(\%N_{ss}) \qquad (2)$$

The second term $\Delta\sigma$ provides material strengthening by precipitation or carbon content in solution. In case of ferrite it is given by

$$\Delta\sigma \text{ (in MPa)} = 5000 * (\%C_{ss}^{f}) \qquad (3)$$

While for martensite it is given by

$$\Delta\sigma \text{ (in MPa)} = 3065 * (\%C_{ss}^{m}) - 161 \qquad (4)$$

Where $\%C_{ss}^{f}$ denotes the wt% carbon content in ferrite and $\%C_{ss}^{m}$ denotes the wt% carbon in martensite.

The third term comprises the effects of dislocation strengthening as well as work softening due to recovery. α is a material constant having a value of 0.33. M is the Taylor factor, and a value of 3 was utilized in this study. μ is the shear modulus and a value of 80000 MPa was applied. b is the Burger's vector and it was taken as a value of $2.5*10^{-10}$ m. k_r is the recovery rate. In case of ferrite a value of $10^{-5}/d_\alpha$ was used, whereas d_α refers to the ferritic grain size. L is the dislocation mean free path.[7, 9] For ferrite, it is equal to the ferritic grain size d_α, while for martensite the values L and k_r were used as fitting parameters.

With respect to the transformation from austenite to martensite during quenching process of the dual phase steel a volume expansion of 3% takes place in the resulted microstructure. This occurrence causes additional dislocations on the phase boundaries due to the hardness difference between transformed martensite and ferrite. On the one hand, the dislocations stored in the vicinity of the boundaries will contribute to forest hardening causing an isotropic hardening. On the other hand, these dislocations will lead to the building up of back stresses giving a kinematic hardening. At low strain values, grain and phase boundaries act as perfectly barriers of dislocations. These dislocations accumulated at the phase boundaries between ferrite and martensite together with the incompatibility between the martensite islands and the ferrite matrix make contributions to a polarized stress. The net polarized stress arising from long range back stress can be expressed in term of the resulting backstress σ_s [10]:

$$\sigma_S = \left[\frac{M\mu b n^*}{d_\alpha}\exp\left(\frac{-\lambda\varepsilon}{bn^*}\right)\left(1-\exp\left(\frac{-\lambda\varepsilon}{bn^*}\right)\right)\right] \qquad (5)$$

It was assumed that efficiency of phase boundary for generating back stresses and for dislocation storage are dictated by the same critical number of dislocations at the boundary n^*. λ is the mean spacing between slip lines at the phase boundaries. For the flow curve of the ferritic phase this kinematic hardening behaviour was additionally taken into account by Eq. (5). The values of n^* and λ were used as fitting parameters.[11] The stress-strain curves of the phase boundary hardening for are depicted in Figure 5 for the DP structures with 25% and 60% martensite.

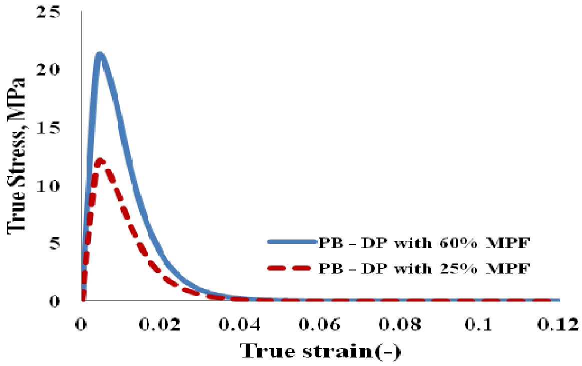

Figure 5 : Stress - strain curves representing phase boundary hardening for DP steels with 25% and 60% martensite.

To obtain plastic flow curves of ferrite and martensite in the RVE, the micromechanical models as discussed were applied [(8)]. The modeled flow curves for ferrite in the investigated DP microstructures with different MPF values are depicted in Figure 6. The discrepancy between the flow curves of ferrite phase in the DP steels annealed at different intercritical temperatures were clearly observed in the strain hardening rate, especially at low strain values. Higher yield strength and strain hardening were obtained for the ferritic phase that exhibits smaller grain size. Note that finer ferrite grains occurred in the DP microstructures with higher martensite fraction. These flow curves of ferrite were later combined with the kinematic hardening term according to phase boundary dislocations for the RVE simulation.

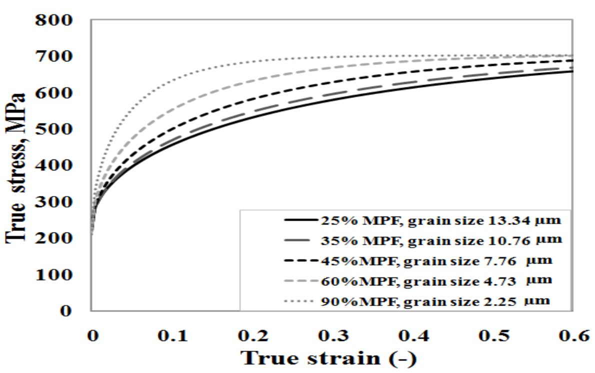

Figure 6 : Modeled flow curves of ferrite in the investigated DP steels having different MPF values and ferritic grain sizes.

The modeled flow curves for martensite are shown in Figure 7. The deviations of the flow curves of martensitic phases in the DP steels annealed at various temperatures are more apparent when comparing with the flow curves for ferrite. The martensite possesses much higher stress than that of the ferrite in all DP microstructures. By this approach, the strain hardening rate of martensite was very high at the beginning of the flow curve. The flow curves reached a saturated value at small strain values. This flow behaviour represented a more brittle manner of the martensite. Higher yield and tensile strengths were observed for the martensite with higher carbon contents. In the DP steels with lower MPF values, the carbon content in martensite is higher according to the rule of mass balance. This significantly led to much increased strength of the martensitic phase.

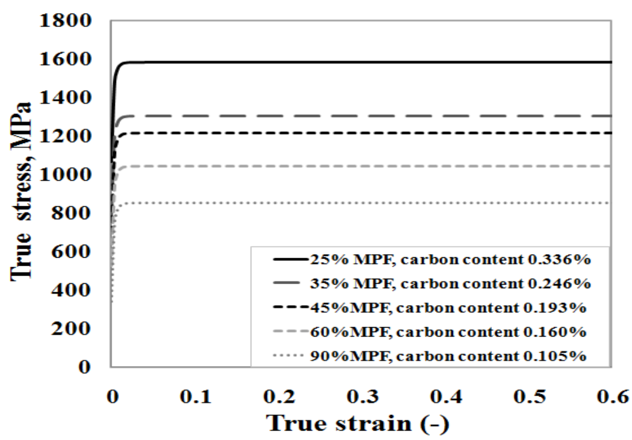

Figure 7: Modeled flow curves of martensite in the investigated DP steels having different MPF values and carbon content.

Result and Discussion

Comparisons of Experimental and Numerical Flow Curves

FE simulations of the 2D RVE model were performed under uniaxial deformation condition using the introduced flow curve models. The arithmetic mean of calculated stress and strain values from the RVE provided the overall properties of material. From the simulations, overall stress-strain curves were determined for different DP microstructures. These results were compared with the experimental stress-strain curves from quasi-static tensile tests for the corresponding DP structures, as shown in Figure 8. The prediction of the flow curves was acceptable, especially for the case of low martensite phase fractions. In case of higher martensite fractions, larger deviations occurred. However, the strain hardening rate could be correctly described for all DP structures, except for the MPF of 90%. It should be noted that in case of the DP steel with high MPF and low carbon content in martensite the overall stress-strain response was more affected by the martensite. The predicted curve exhibited low strain hardening rate at strain beyond 0.01 similar to the flow curve of martensite and therefore underestimated the experimental curves. In the modeling, strain hardening model for the martensitic phase in the DP steel with high MPF should be differed from the one in the DP steel with low MPF. First, morphologies of martensite in the DP steel with high and low MPF were unlike. Secondly, martensites in both DP steels contained different carbon contents, which are directly related to the hardness of the martensitic phase. The effect of the kinematic hardening due to the phase boundary dislocations could be seen at the beginning of the flow curves, where good agreements with the experimental results were observed. Nevertheless, the calculations were based on 2D plain strain assumption. A 3D calculation should provide a more precise prediction.

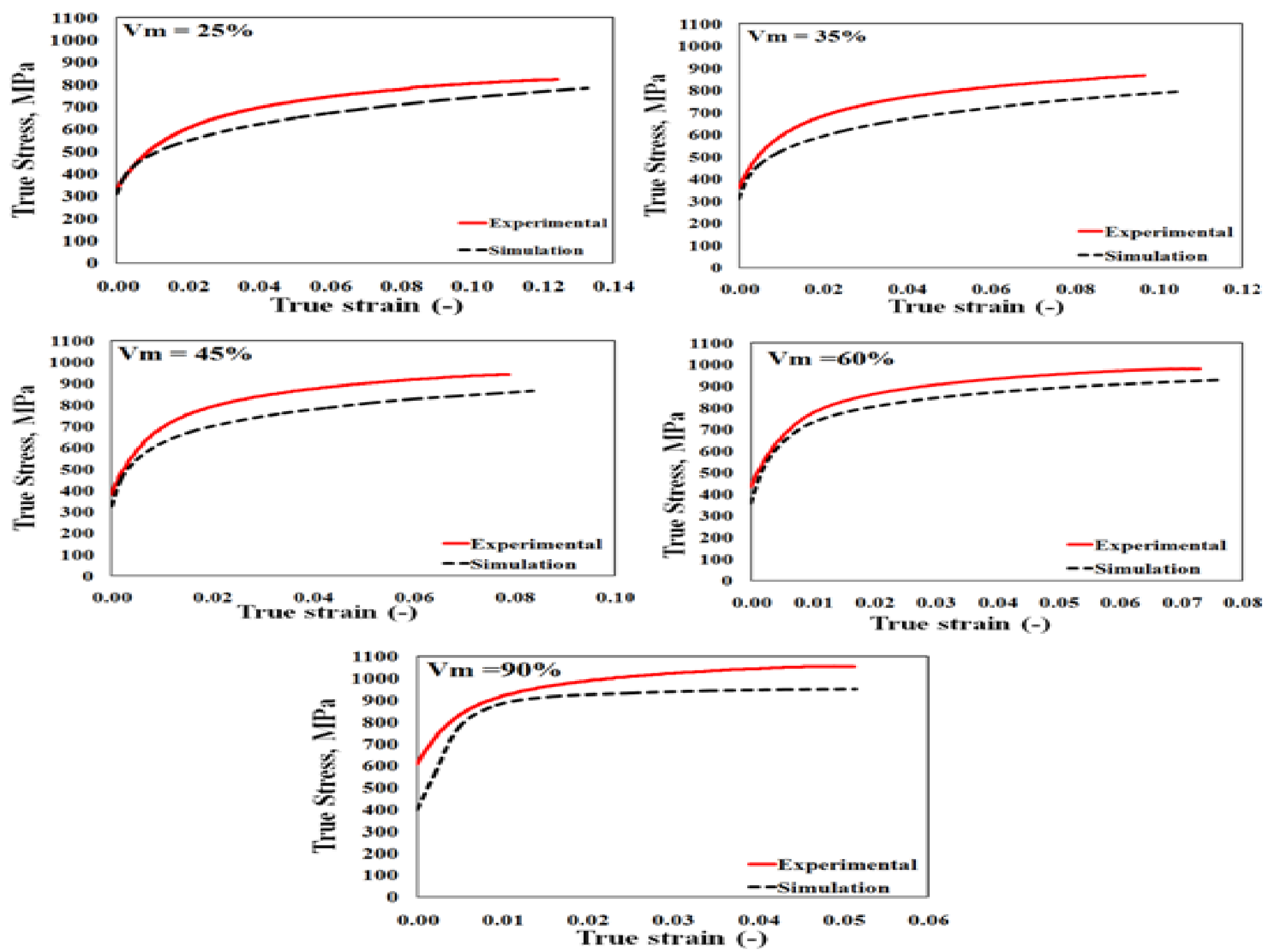

Figure 8: Comparisons between experimental and numerical flow curves of the investigated DP steels with varying martensite contents.

Local Stress-Strain Distribution

In the 2D RVE model real morphologies and microstructural constituents of the DP steel were considered on the micro - level. The evolution of local stress and strain in the DP microstructures was obtained from the RVE simulations. Distribution of equivalent Von Mises stress in the DP microstructure consisting of 25% and 60% martensite phase fraction after a macroscopic uniaxial tensile deformation of 10% was illustrated in Figure 9 (a) and 9 (b), respectively. Obviously, in the DP microstructure consisting of 60% martensite higher stresses mostly developed along the interfaces between ferrite and martensite. The stress distribution was more uniform in the DP microstructure with lower MPF due to the more finely dispersed martensite islands. The local plastic strain distribution was also determined and localized bands occurring on the direction of 45° to the tensile loading direction were observed, as depicted in Figure 10. Many short interrupted shear bands were found in the DP structure consisting of 25% martensite, but long continuously localized bands appeared in the DP structure consisting of 60% martensite. The localization or shear bands occurred in the DP microstructure during the deformation strongly depended on the martensite morphology. The lower elongation of the DP steel consisting of 60% martensite could be also explained by this phenomenon, in which the microstructure tended to have long localized bands occurred earlier, though martensite in the DP steel with 60% MPF was weaker and less brittle than martensite in the DP steel with MPF of 25% due to different carbon contents.

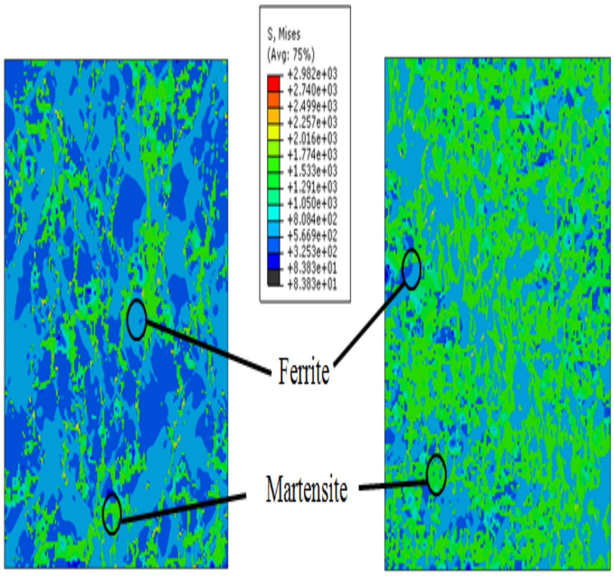

Figure 9: Local stress distribution in the DP microstructure with (a) MPF of 25% (b) MPF of 60% at uniaxial tensile strain of 10%.

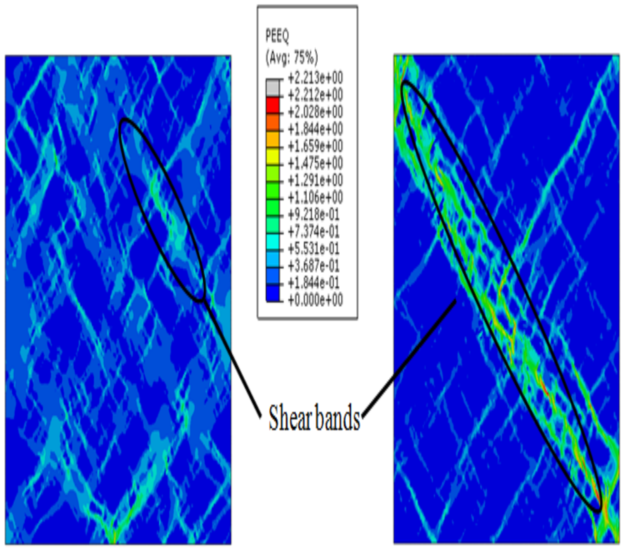

Figure 10: Local strain distribution in the DP microstructure with (a) MPF of 25% (b) MPF of 60% at uniaxial tensile strain of 10%.

Conclusion

In this work, different intercritical temperatures were applied during annealing process in order to generate the DP steel containing different martensite phase fractions between 25% and 90%. The microstructures of the produced DP steels were characterized by LOM and uniaxial tensile test. It was found that the microstructures of the DP steels contained globular and irregular martensite surrounded by ferritic matrix. The yield and ultimate tensile strength of the DP steels were increased with increasing MPF, but the elongation was reduced. In addition, a microstructure based FE modeling was performed to predict plastic flow curves of the investigated DP steels. 2D RVE was generated using real micrographs and FE RVE simulations were carried out under uniaxial tensile deformation. The results regarding prediction of the stress-strain responses were acceptable. The modeled flow curves for martensite showed very high strain hardening at the beginning and then reached a saturated stress. This behaviour could lead to underestimated results for the DP steel with higher MPF. The DP steel with higher MPF exhibited higher overall strength but lower ductility, though the carbon content in martensite was lower and the martensite was thus weaker. The mechanical properties of DP steel are strongly influenced by morphology of the dispersed martensitic phase. The modeling approach can be further developed and used for describing deformation and failure behaviour of the multiphase high strength steels.

Acknowledgement

This research work has been financially supported by the National Metal and Materials Technology Center, Thailand (MTEC).

References

1. Final Report USLAB (1998). Ultra light steel auto body. *American Iron and Steel Institute, Washington, DC*.

2. Rashid, M.S**.** (1981). Dual phase steels. *Ann. Rev. Mater. Sci.* **(11) :** 245-266.

3. World Auto Steel (2009). Advanced high strength steel (AHSS) application guidelines, *URL:* *http:// www.worldautosteel.org* access on 15/03/2009.

4. Park, K.S., Park, K.T., Lee, D.L., Lee, C.S. (2007). Effect of heat treatment path on the cold formability of drawn dual-phase steels. *Mater. Sci. Eng. A* **(449-451):** 1135–1138.

5. Ramazani, A., Mukheriee, K., Prahl, U., Bleck, W. (2012). Modelling the effect of microstructural banding on the flow curve behavior of dual-phase (DP) steels. *Comp. Mater. Sci.* **52(1):** 46-54.

6. Albbasi, F. (2004). Micromechanical modeling of dual phase steels. *PhD Thesis, McGill University, Montral, Canada*.

7. Rodriguez, R.M., Gutierrez, I. (2003). Unified formulation to predict the tensile curves of steels with different microstructures. *Mater. Sci. Forum* **(426-432):** 4525-4530.

8. Bouaziz, O., Buessler, P. (2002). Mechanical behavior of multiphase materials: An intermediate mixture law without fitting parameter. *La Revue de Metallurgie* **(99):** 71-77.

9. Uthaisangsuk, V., Prahl, U., Bleck, W. (2008). Micromechanical modelling of damage behaviour of multiphase steels. *Comp. Mater. Sci.* **(43):** 27-35.

10. Delince, M., Brechet, Y., Embury, J.D., Geers, M.G.D., Jacques, P.J., Pardoen, T. (2007). Structure–property optimization of ultrafine-grained dual-phase steels using a microstructure based strain hardeningmodel. *Acta Materialia* **(55):** 2337–2350.

11. Sinclair, C.W., Poole, W.J., Brchet, Y. (2006). A model for the grain size dependent work hardening of copper. *Scripta Materialia*. **(55):**739-742.